

Article

# Mechanical Properties of Tin Slag Mortar

Nathaniel Olukotun <sup>1,2,\*</sup>, Abdul Rahman Mohd Sam <sup>1,3</sup>, Nor Hassana Abdul Shukor Lim <sup>1</sup>,  
Muyideen Abdulkareem <sup>4</sup>, Isa Mallum <sup>1,5</sup> and Olukotun Adebisi <sup>6</sup>

<sup>1</sup> School of Civil Engineering, Universiti Teknologi Malaysia, Johor 81310, Malaysia; abdrahman@utm.my (A.R.M.S.); norhasanah@utm.my (N.H.A.S.L.); misa@graduate.utm.my (I.M.)

<sup>2</sup> Department of Building Technology, Kogi State Polytechnic, Lokoja 270103, Nigeria

<sup>3</sup> Construction Research Centre, Universiti Teknologi Malaysia, Johor 81310, Malaysia

<sup>4</sup> Department of Civil Engineering, Faculty of Engineering, Technology and Built Environment, UCSI University, Kuala Lumpur 56000, Malaysia; abdulcareem@ucsiuniversity.edu.my

<sup>5</sup> Department of Civil Engineering Technology, Adamawa State Polytechnic, Yola 640231, Nigeria

<sup>6</sup> Department of Civil Engineering, University of Abuja, Abuja 900108, Nigeria; olukotunadebisi@gmail.com

\* Correspondence: olukotunnathaniel78@gmail.com

**Abstract:** The increased demand for cement mortar due to rapid infrastructural growth and development has led to an alarming depletion of fine aggregate. This has prompted the need for a more sustainable material as a total/partial replacement for natural fine aggregate. This study proposes the use of tin slag (TS) as a replacement for fine aggregate in concrete to bridge this sustainability gap. TS was used to replace fine aggregate at replacement levels of 0%, 25%, 50%, 75%, and 100% in cement mortar. Fresh and hardened properties of TS mortar were obtained. Flow tests showed that, as the TS quantity and the  $w/c$  ratio increased, the mortar flow increased. Similarly, the compressive strength increased as the TS replacement increased up to 50% replacement, after which a decline in strength was observed. However, with the TS replacement of fine aggregate up to 100%, a compressive strength of 6% above control was attained. The morphological features confirm that specimens with TS had a denser microstructure because of its shape characteristics (elongated, irregular, and rough), and, thus, plugged holes better than the control mortar. The natural sand's contribution to strength was a result of better aggregate hardness as compared to TS. Hence, TS can be used as alternative for fine aggregate in sustainable construction.

**Keywords:** tin slag; mortar; compressive strength; fine aggregate; rough surfaced; elongated



**Citation:** Olukotun, N.; Sam, A.R.M.; Lim, N.H.A.S.; Abdulkareem, M.; Mallum, I.; Adebisi, O. Mechanical Properties of Tin Slag Mortar. *Recycling* **2021**, *6*, 42. <https://doi.org/10.3390/recycling6020042>

Academic Editors: José Neves and Ana Cristina Freire

Received: 15 January 2021

Accepted: 31 March 2021

Published: 21 June 2021

**Publisher's Note:** MDPI stays neutral with regard to jurisdictional claims in published maps and institutional affiliations.



**Copyright:** © 2021 by the authors. Licensee MDPI, Basel, Switzerland. This article is an open access article distributed under the terms and conditions of the Creative Commons Attribution (CC BY) license (<https://creativecommons.org/licenses/by/4.0/>).

## 1. Introduction

Concrete is the most utilized material after water. Consequently, its demand has been on the rise at a rate of 5% annually. It is estimated that about 25 to 30 billion tons of concrete are manufactured globally every year [1]. This amount of produced concrete suggests that its constituents are exploited in huge volumes. This may further increase because of population explosion, unprecedented growth, and global industrialization. Fine aggregate constitutes about 30% of the volume of concrete. There are no exact measures on the quantity of fine aggregates available for use worldwide or by country. However, from 2018 estimates of cement consumed worldwide, about 8 billion tons of fine aggregate is consumed yearly [1]. It has been reported that the rate of depletion is faster than its renewal, and the consumption rate increases every year. In addition, natural sand is utilized for the production of glass and electronics and for road construction.

Reducing the consumption of natural sand by looking for alternative materials for its replacement is important. Lately, crushed and manufactured sand have been used as alternatives to natural fine aggregate (NFA) [2,3]. However, the crushing and manufacturing process is capital intensive. Many studies have been conducted to establish new substitutes for NFA by utilizing industrial waste materials such as steel slag [4], lead slag [5], copper slag [6], foundry sand [7], and recycled glass [8]. This reduces the dependence on natural

sand and propels the sustainability of this declining resource. For example, Zhao et al. (2018) replaced 20% of fine aggregate in concrete with steel slag. The replacement showed that compressive strength was improved by 28% over the control concrete sample. Similarly, copper slag was used up to 100% as a fine aggregate replacement by Prem et al. (2018) [6]. It was observed that 100% copper mortars had a 3% compressive strength above the control mortar replacement. The use of foundry sand and recycled glass at 10% replacement has also been found to improve the mechanical properties of concrete [9,10].

Another such industrial waste readily available and under-utilized is tin slag (TS). TS is a by-product obtained from the production of tin. About 2 million tons of TS waste is available at landfills worldwide [11]. Very few studies have been conducted on the use of TS as a fine aggregate replacement. Shakil and Hassan [12] evaluated the properties of TS polyester polymer concrete. The compressive strength test showed that samples attained a strength of 125.07 MPa. Hashim et al. [13] applied TS as a replacement of fine aggregate to produce interlocking pavement bricks. The study showed that the compressive strength increased by 20%, however, the study considered only 100% and 20% TS replacement of fine aggregate. Rustandi et al. (2018) [14] utilized the pozzolanic properties of TS by replacing 10% of the cement. The TS mortar achieved only a 63% compressive strength of the control sample at 28 days.

This study examines the utilization of TS as a replacement of NFA in cement mortar. Five different replacement fractions of TS (0%, 25%, 50%, 75%, and 100%) were introduced into the mortar mixes as replacements of fine aggregate. This was done using different water/cement ( $w/c$ ) ratios of 0.5, 0.55, and 0.6. The specimens were prepared, and tests were conducted at fresh and hardened states. Tests were conducted after 3, 7, and 28 days of water-curing the specimens. The workability of the mortar was measured by the flow table test to evaluate the effect of TS on the flowability of TS mortars. The mechanical properties measured were compressive strength, flexural strength and tensile strength

## 2. Experiment

### 2.1. Materials

The materials used in this study were cement, NFA, TS, and water. TS was used as a replacement material of fine aggregate in different weight fractions. Ordinary Portland cement (OPC) with a gauge of 42.5 and a specific gravity of 3.14 according to ASTM C (American Standard Testing Methods) 150 [15] was used. NFA and TS of a 4.75 mm maximum aggregate size were used. The TS used was obtained from the tin smelting company in Penang, Malaysia. Tap water was used for the mixing and curing of the mortar specimens. The physical and chemical properties of the fine aggregate were measured according to ASTM C128 [16] and presented in Tables 1 and 2. The shape characteristics showed that the fine aggregate particles were round and smooth, whereas the TS particles were elongated and rough-surfaced. TS particles at the macro state are depicted in Figure 1.

### 2.2. Particle Size Gradation

The grading of aggregates was done in conformity to ASTM C33 [17] protocols. The initial sieve analysis performed for TS aggregate indicated that it did not conform to ASTM requirements, as shown in Figure 2. About 50% of the aggregate fell within the 4.75 to 2.36 mm range. The grading method used was to separate the aggregate passing through different sieves and thereafter combine the appropriate percentage allowed of each size according to ASTM standards. The aggregates were thoroughly mixed and a second sieve analysis was conducted. Figure 3 shows the chart of the second sieve analysis. Large aggregates (4.75–2.36 mm) that were in excess were grinded in a ball mill machine to reduce their sizes and were thereafter re-graded. This was necessary to ensure that aggregates were efficiently utilized and that wastage avoided. About 2% of aggregates were discarded.

**Table 1.** Physical properties of fine aggregate and tin slag (TS).

S/N	Physical Properties	Sand	TS
1	Specific gravity	2.62	3.0
2	Water absorption	2.0	1.98

**Table 2.** Chemical properties showing major oxides of fine aggregate and tin slag.

S/N	Chemical Properties	Sand	TS
1	Silica	91.5	15.8
2	Alumina	3.55	7.10
3	Magnesium oxide	1.3	0.85
4	Iron oxide	1.2	33.4
5	Calcium oxide	0.5	21.3
6	Titanium(IV) oxide	-	5.74
7	Zirconium oxide	-	2.16
9	Niobium(V) oxide	-	1.36
10	Tin(IV) oxide	-	1.62
11	Tantalum(V) oxide	-	1.31
12	Tungsten(VI) oxide	-	3.08



**Figure 1.** The macro morphology of tin slag.

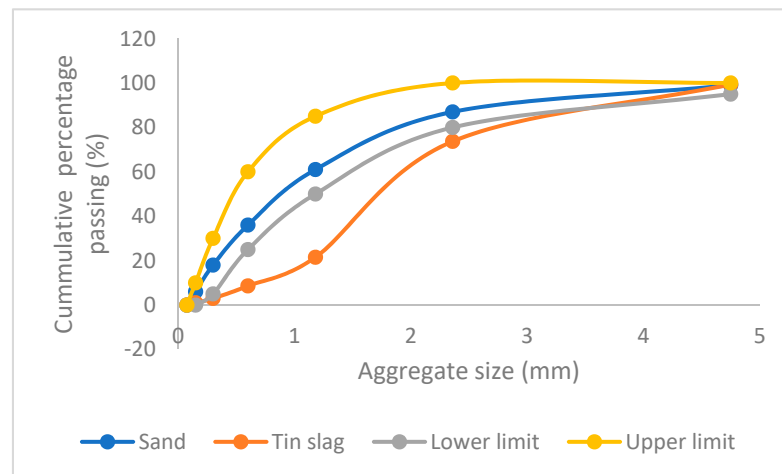


**Figure 2.** Initial sieve analysis.

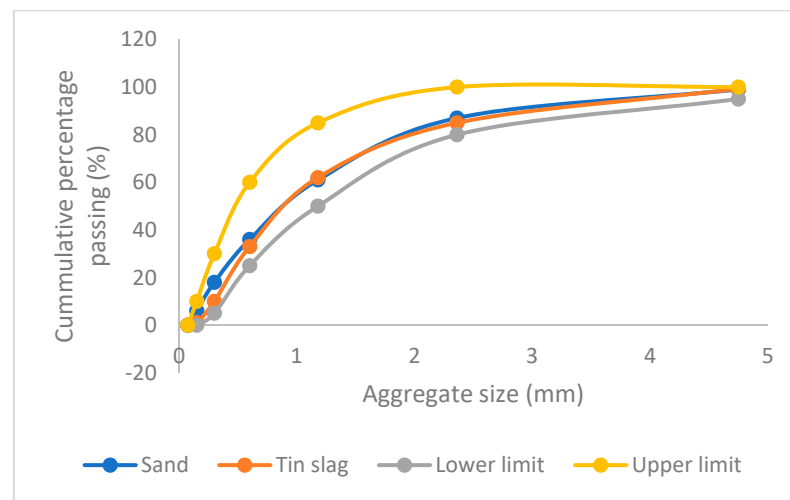


Figure 3. Second sieve analysis.

### 2.3. Mix Proportioning and Sample Preparation

Fifteen different mixes were prepared for this study. All mortar specimens were prepared using a cement to fine aggregate volume ratio of 1:3. The control mix sample was NFA-based, while the other samples had 25%, 50%, 75%, or 100% of the fine aggregate replaced with TS. The TS percentage replacement levels of fine aggregate are shown in Table 3. The control sample (TS0) contained a 0% TS replacement of fine aggregate, whereas TS100 contained a 100% TS replacement of fine aggregate. The *w/c* ratios applied in this study were 0.5, 0.55, and 0.6.

Table 3. The mix percentages of tin slag (TS) in mortar.

Designation	Fine Aggregate (%)	Replacement Levels of TS (%)
Control (TS0)	100	0
TS25	75	25
TS50	50	50
TS75	25	75
TS100	0	100

It should be noted that the TS used in this study had a specific gravity of 14.5% above that of NFA. Therefore, multiplication factors (shown in Table 4) were applied to obtain the correct corresponding TS mass percentage replacement of fine aggregate. These multiplication factors were applied so that aggregate volumes of different mortar mixes (TS0, TS25, TS50, TS75, and TS100) were the same, despite the difference in the specific gravities of the NFA and the TS. The multiplication factors were derived from the densities of the aggregates (natural sand and TS) used for the different mixes. For example, the multiplication factor for TS25 = the density of the combined aggregates (75% NFA and 25% TS)/the density of the NFA. The constituent quantity of each mix sample is given in Table 5. To reduce error in this study, three specimens were produced for each mix proportion, and the average was taken. In this study, 135 cubes were prepared for compressive strength tests, while 45 cylinders and 45 prisms were prepared for splitting tensile and flexural strength tests, respectively. In addition, 45 mortar bars were prepared for ASR (Alkali silica reaction) tests. Demolding was done after 24 h and samples were cured in water for 3-, 7-, and 28-day periods.

**Table 4.** The Multiplier factors for tin slag mortars.

Designation	Multiplier Factor
TS25	1.06
TS50	1.12
TS75	1.16
TS100	1.20

**Table 5.** The mix proportions of constituents for 1 m<sup>3</sup> of mortar.

Mix	Designation	Cement (kg)	Sand (kg)	Tin Slag (kg)	Water (kg)	w/c
M1	TS0	530	1590	0	265	0.5
M2	TS25	530	1192.5	421	265	0.5
M3	TS50	530	795	890	265	0.5
M4	TS75	530	397.5	1383	265	0.5
M5	TS100	530	0	1908	265	0.5
M6	TS0	530	1590	0	291.5	0.55
M7	TS25	530	1192.5	421	291.5	0.55
M8	TS50	530	795	890	291.5	0.55
M9	TS75	530	397.5	1383	291.5	0.55
M10	TS100	530	0	1908	291.5	0.55
M11	TS0	530	1590	0	318	0.6
M12	TS25	530	1192.5	421	318	0.6
M13	TS50	530	795	890	318	0.6
M14	TS75	530	397.5	1383	318	0.6
M15	TS100	530	0	1908	318	0.6

#### 2.4. Testing Procedures

Several tests were carried out on the TS cement mortar and control samples to evaluate the effects of the replacement of fine aggregate with TS. These involved the fresh and hardened states of the samples. The fresh property considered in this study was workability, and this was performed through a mortar flow test in accordance to ASTM C 1437 [18] guidelines.

The hardened properties measured were compressive strength, tensile strength, flexural strength, and alkali–silica reactivity. The compressive strength was measured using a 3000 kN compression testing machine in accordance to ASTM C109 [19] procedures. Cube dimensions of 50 × 50 × 50 mm<sup>3</sup> were used in this experiment. The tensile strength test was performed according to ASTM C 496 [20] guidelines. Samples used for tensile strength tests were 70 mm (diameter) × 150 mm (length) cylinders. Testing was done with plywood strips positioned perpendicular to diametral lines drawn on the specimens.

The flexural strength testing, on the other hand, was performed according to ASTM 348 [21]. The specimens applied for the flexural test had dimensions of 40 × 40 × 160 mm<sup>3</sup>. Figure 4 shows the hardened state tests (compressive, tensile, and flexural tests). Additionally, the alkali–silica reactivity check was performed according to ASTM C1567. This test was performed to determine the level of reactivity of the TS aggregate in the mortar. This was necessary because of the presence of CaO in TS, as shown in Table 2. The phase diagram of grounded TS (Figure 5) shows that it has a dominant amorphous phase with few crystalline peaks. The specimens used were 25 × 25 × 250 mm<sup>3</sup> mortar bars.

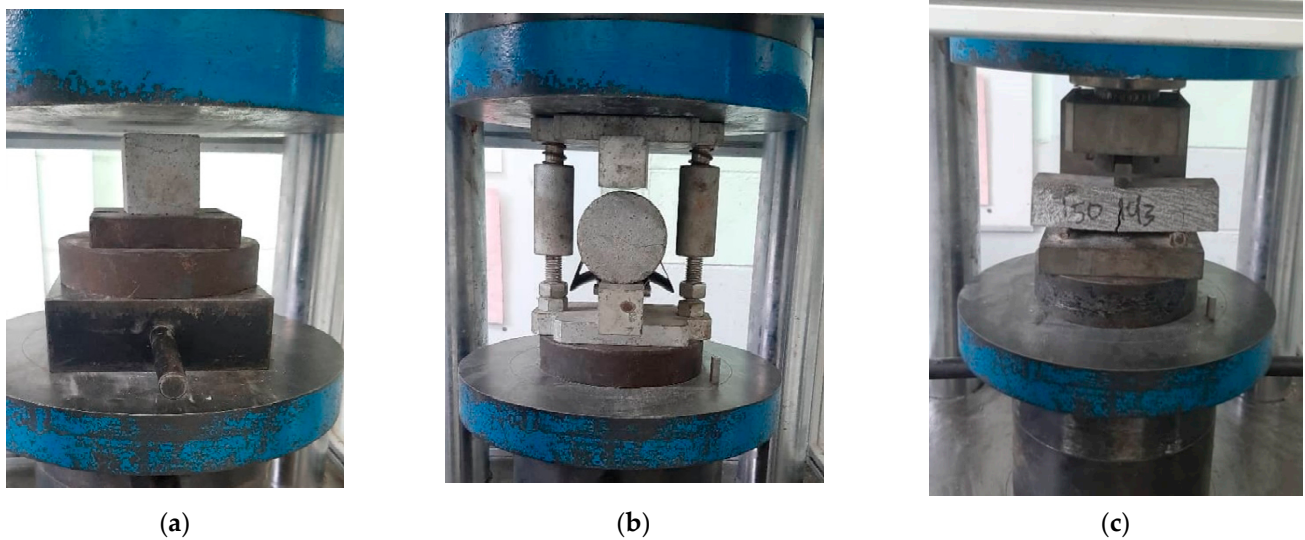


Figure 4. Hardened state tests: (a) the compression test, (b) the split tensile test, and (c) the flexure test.

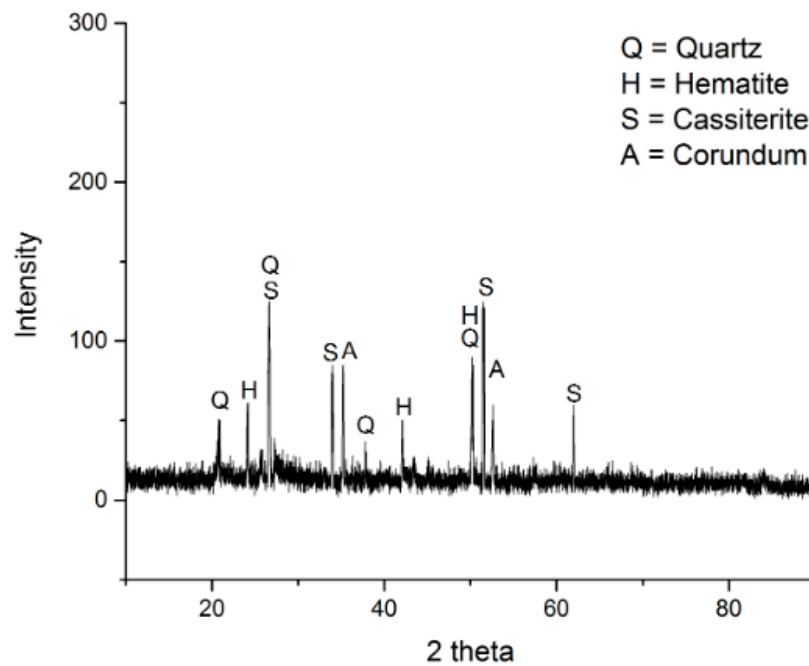


Figure 5. XRD (X-ray diffractometer) pattern of tin slag aggregate [14].

### 3. Experimental Results

#### 3.1. Workability

Workability is the property of mortar that allows for adequate compaction, placement, and finish without segregation and/or bleeding. The flowability for all samples containing graded and non-graded particles were measured by the flow cone test. Figure 6 illustrates the mortar flow after the flow cone tests. As can be seen, normal and scattered flows were observed. All samples of graded and ungraded TS mortars exhibited normal flow, except ungraded TS100 mortars of  $w/c$  ratios of 0.5 and 0.55. The flow test results for the ungraded and graded particles are presented in Figures 7 and 8.



Figure 6. Mortar consistencies: (a) normal flow and (b) scattered flow.

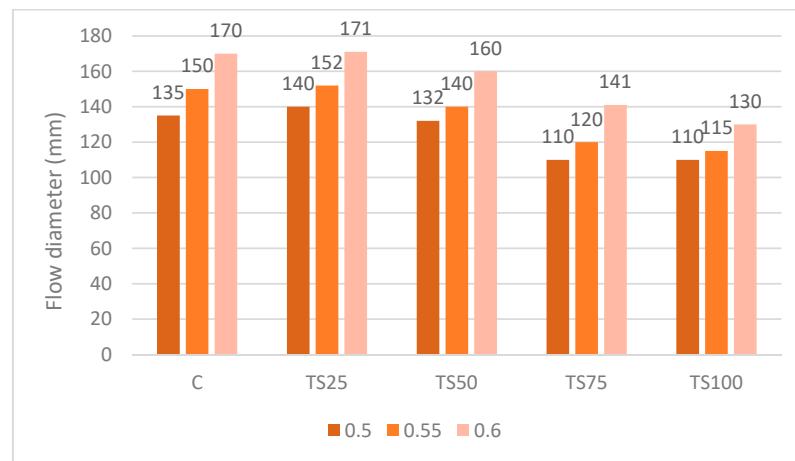


Figure 7. Flow diameters of ungraded TS at different  $w/c$  ratios.

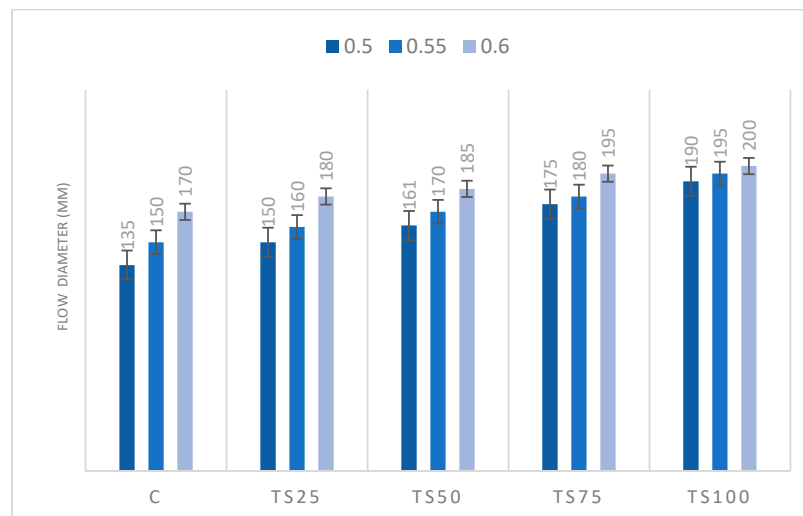


Figure 8. Flow diameters of graded TS at different  $w/c$  ratios.

Figure 7 indicates that the workability of ungraded TS mortar marginally increased up to a 25% replacement, but, thereafter, a downward trend were observed for TS50, TS75, and TS100 mortars.

The workability of the control sample and of TS25 was 170 mm and 171 mm, respectively, at a  $w/c$  ratio of 0.6. As the percentage of ungraded TS increased, the workability of the TS mortar decreased, provided that the  $w/c$  ratio remained the same. For example, at a  $w/c$  ratio of 0.6, the workability increased from 170 mm to 171 mm for TS0 and TS25, and afterwards decreased to 160 mm, 141 mm, and 130 mm for TS50, TS75, and TS100 mortars, respectively. This effect is attributed to particle interference, which increasingly occurred as TS replacement increased. The larger particles (2.36–4.5 mm) were more prominent smaller particles (Figure 2). Thus, pockets of spaces narrower than the diameter of the smaller particles were created. These spaces trapped water that would have provided better consistency, thereby increasing the water demand [22]. In addition, due to the lack of smaller particles in the ungraded TS, the ball bearing effect by smaller particles (which is needed to lubricate larger particles) was reduced as TS replacement increased [23]. This trend was noticed at  $w/c$  ratios of 0.5 and 0.55, except regarding the TS 100 mortar, for which a scattered flow was observed. The mortar flow diameter does not give an accurate representation of flow. The scattered flow was attributed to inadequate cohesion between TS aggregates within the matrix, which is due to insufficient water for mixing [24]. Pockets of spaces created by the ungraded TS used up part of the mixing water. Figure 8 shows that the workability of graded TS mortar increased as the quantity of TS increased [25,26]. For example, the workability of graded TS mortar increased from 135 to 190, as the quantity of TS increased from 0 to 100% at a  $w/c$  ratio of 0.5. Cumulative increases of 10 mm, 15 mm, 30 mm, and 35 mm above the control were noticed for TS25, TS50, TS75, and TS100 mortars. The same trend was noticed at a  $w/c$  ratios of 0.55 and 0.6.

From Figures 7 and 8, it can be observed that higher  $w/c$  ratio yielded increased workability, both for graded and ungraded TS samples. For example, when the  $w/c$  ratio of the ungraded TS was increased from 0.5 to 0.6 at TS50, the workability increased from 132 mm to 160 mm, while an increase from 161 mm to 185 mm was observed for graded TS samples. This was due to an increase in water for the mixing constituents as the water content increased. However, in terms of shape and texture, round and smooth particles have better workability than elongated or angular particles [23,27]. Nonetheless, it was observed that graded TS mortars had higher flow diameters than ungraded TS mortars. This was attributed to the low water absorption of TS, which promoted water retention which improved lubrication between particles. Thus, the effect of yield stress and water demand resulting from the angular shape characteristics of TS was insignificant [28].

### 3.2. Alkali–Silica Reactivity

Figure 9 shows the result of the alkali–silica reaction test of samples in this study. The expansion of TS mortars at different replacement levels are presented. The drying shrinkage of TS100 mortars were just fractionally lower than the control. Thus, the differential effects on these mortars are insignificant. The shrinkage values of mortars at 14 days for TS25, TS50, TS75, and TS100 were 0.009%, 0.008%, 0.0096%, and 0.0097%, respectively, compared to the control specimen (TS0) value of 0.01%. The T50 mortar had the lowest expansion of 0.08%. The lower rate of expansion of TS mortars was attributed to the rough texture and angularity of aggregates, which provided a denser microstructure. This has been reported by other researchers [29,30]. However, the contribution of the fine aggregate's hardness contributed to the compactness observed in TS50 mortars. Overall, all mortars had comparable results and were within the ASTM [31] expansion limit of 0.1%; therefore, TS aggregate is non-reactive.



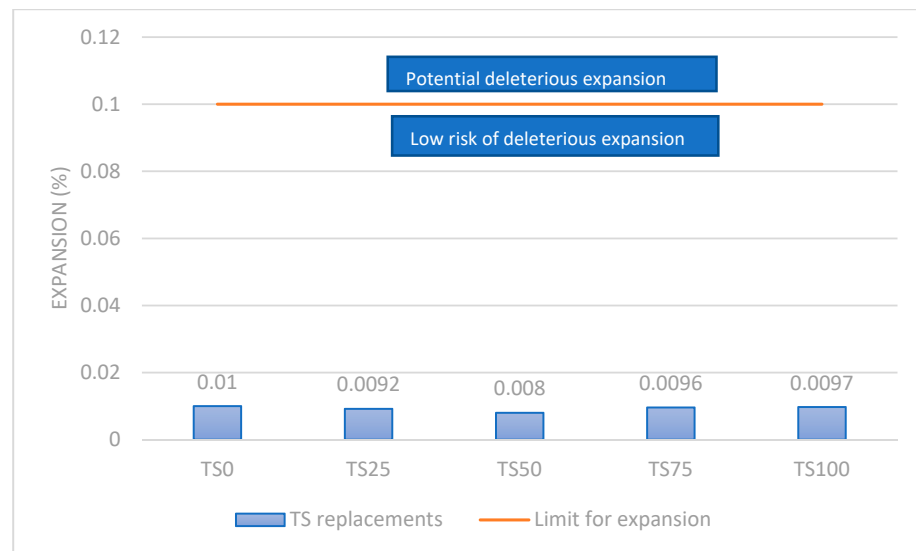


**Figure 9.** The expansion of the mortars at 14 days.

### 3.3. Compressive Strength

In this section, the 28-day compressive strength of graded TS mortars with different  $w/c$  ratios are presented and compared to the control sample. In addition, the compressive strengths of the TS cement mortar and control samples obtained at days 3, 7, and 28 are presented to check the early strength of the TS cement mortar samples. Figure 10 shows the 28-day compressive strength of mortar mixes at different  $w/c$  ratios. In all samples (control and TS), It was observed that, as  $w/c$  increased, the compressive strength decreased. The compressive strength decreased by as much as 25% due to the increased  $w/c$  ratio. For example, at TS50, the compressive strength decreased from 45.42 MPa to 34.22 MPa when the  $w/c$  ratio increased from 0.5 to 0.6. This result is consistent with previous findings [32,33]. However, to achieve good workability, mortars must not exhibit segregation or bleeding. Samples with a  $w/c$  ratio of 0.5 had the highest compressive strength but were too stiff; thus, their use is not practicable. Additionally, mortars with a  $w/c$  ratio of 0.6 were most workable, but segregation and bleeding were noticed, as was low compressive strengths (Figure 6). Contrarily, bleeding and segregation did not occur in mixes with a  $w/c$  ratio of 0.55. Thus, mortar mixes containing a water to binder ratio of 0.55 were selected based on their workability and strength. Compressive strength development is presented in Figure 11. However, both ungraded and graded TS mortar samples were tested for compressive strength to evaluate the influence of grading, as workability results showed differing trends (as shown in Figures 7 and 8).

Figure 11 shows the compressive strength development of mortar samples with a  $w/c$  ratio of 0.55 after 28-days of curing. All fine aggregate replacements with graded TS increased the compressive strength of cement mortar on all curing days (3, 7, and 28). For example, the 3, 7, and 28 days compressive strengths of the control sample were 25.43 MPa, 33.87 MPa, and 38.75 MPa, respectively, whereas the TS samples' lowest values were 26.35 MPa, 34.5 MPa, and 40.2 MPa, respectively. The increase in strength was due to the improved bonding provided by the TS's aggregate angularity and surface roughness. Furthermore, as TS increased in the cement mortar, the compressive strength also increased. This compressive strength increase peaked at 50% replacement (TS50), while further increase in TS quantity decreased the compressive strength of the TS mortar. For example, at 28 days, when TS increased from 25% (TS25) to 50% (TS50), the compressive strength increased from 40.2 MPa to 43.15 MPa. Thereafter, this value decreased to 42.99 MPa and 41.12 MPa as TS increased to 75% (TS75) and 100% (TS100), respectively. The decrease in compressive strength is attributed to the reduction of aggregate hardness as TS% increased to 75% and 100% [34].



Figure 10. The compressive strength of graded TS at different  $w/c$  ratios.

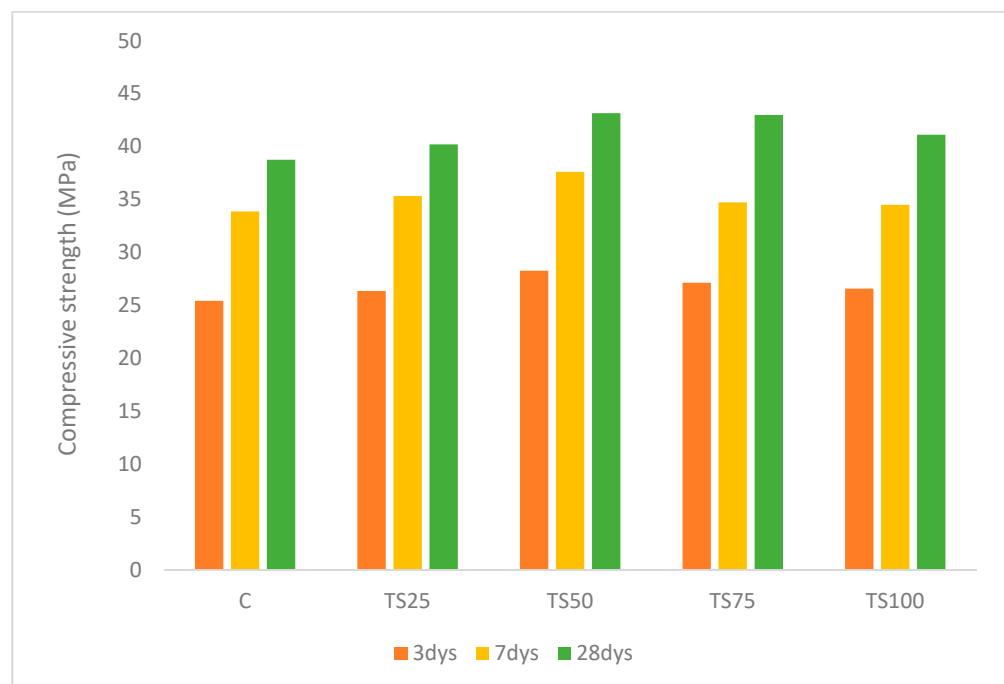
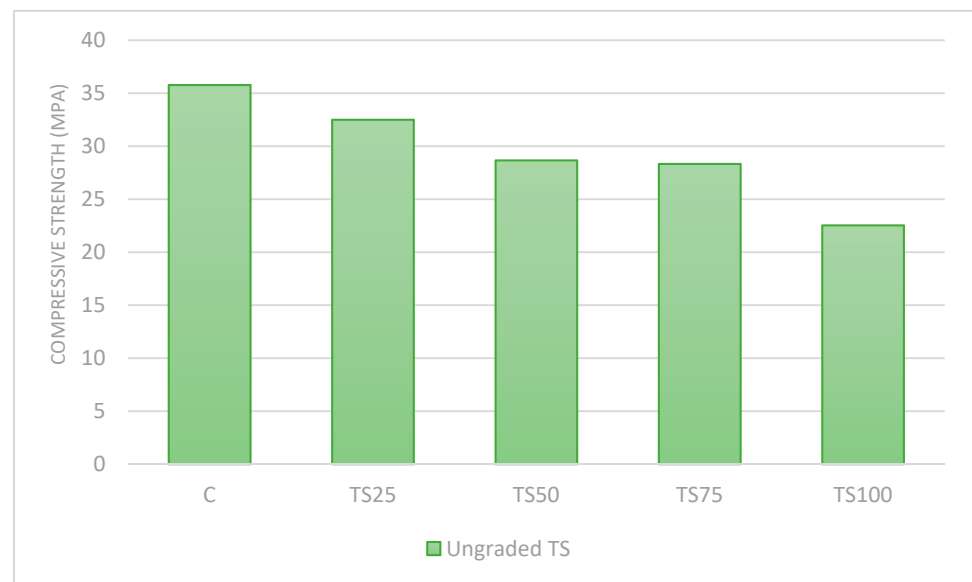


Figure 11. The compressive strength development of graded TS mortars at a  $w/c$  of 0.55.

Compressive strength was improved because of the densification of TS mortars, which is linked to TS’s rough surface structure and the well-bonded interfacial transition zone (ITZ) of TS mortars. Better adherence was expected for rough-surfaced materials compared to smooth-surfaced fine aggregate. The elongated and angular shape of the TS aggregate also contributed to the filling pores between the TS mortar a greater extent than the control mortars. The elongation of TS aggregates allowed a greater depth of embedment while their angularity improved the bond within the matrix. Similar results were reported by Ouda and Abdel-Gawwad [35] and Guo et al. [36]. Ouda and Abdel-Gawwad observed that the rough surface and angularity of oxygen furnace slag aggregate are attributed to the

progressive contribution of strength up to 100% replacement. Likewise, Guo et al. indicated that the rough surface and angularity of steel slag resulted in a higher bonding strength. On the other hand, the contribution of natural sand was attributed to the hardness of the natural sand aggregate as compared to the TS. Thus, the combined effect of the fine aggregate strength of natural sand and the good adherence and bonding characteristics of the TS aggregate provided the optimum strength recorded at 50% replacement. Conversely, when the TS content increased above 50%, the contribution of natural sand to compressive strength in terms of hardness reduced. This is because the contribution of natural aggregate reduces while that of TS increases as the amount of TS increases beyond 50%. However, the effects of aggregate hardness and bonding characteristics were optimal at 50% replacement. Thus, the optimum strength was obtained at 50% replacement.

A different trend was observed with the ungraded TS (Figure 12). A progressive reduction in the compressive strength was noticed, even at 50% replacement, which had the highest compressive strength for graded TS.



**Figure 12.** The 28-day compressive strength of ungraded TS mortars at a  $w/c$  of 0.55.

The control mortar had the highest compressive strength of 35.78 MPa, whereas TS25, TS50, TS75, and TS100 had compressive strengths of 32.51 MPa, 28.67 MPa, 28.33 MPa, and 22.54 MPa, respectively. This shows that the effect of the TS aggregate in terms of bond improvement in graded TS was not seen in the ungraded TS. This was due to inadequate distribution of aggregates within the matrix because larger aggregates dominate as TS replacement increases. Consequently, more pores are formed within the matrix and the progressive compressive strength reduces.

Figure 13 shows the strength development in graded and ungraded samples. An upward trend was observed with graded TS and a downward trend for ungraded TS samples. The increase in strength noticed in the graded TS mortar was attributed to improved packing density, as smaller aggregates fill pore spaces between larger aggregates. This was affirmed in Li et al. [37]. It was observed that packing density is a major factor that influences the compressive strength behavior of cement composites. The compactness of composites produced from mixed aggregates slows down crack propagation because of improved packing density as pore spaces are filled by smaller aggregates. This results in a smaller number of cracks and crack diameters, as compared to uniform or ungraded aggregates. On the other hand, in ungraded samples, a progressive reduction in compressive strength was noticed as TS replacement increased. This was credited to the progressive increase in particle interference due to the increasing number of larger particles. Thus,

packing density was not optimized, so a larger number of pores and, consequently, a low compressive strength resulted.

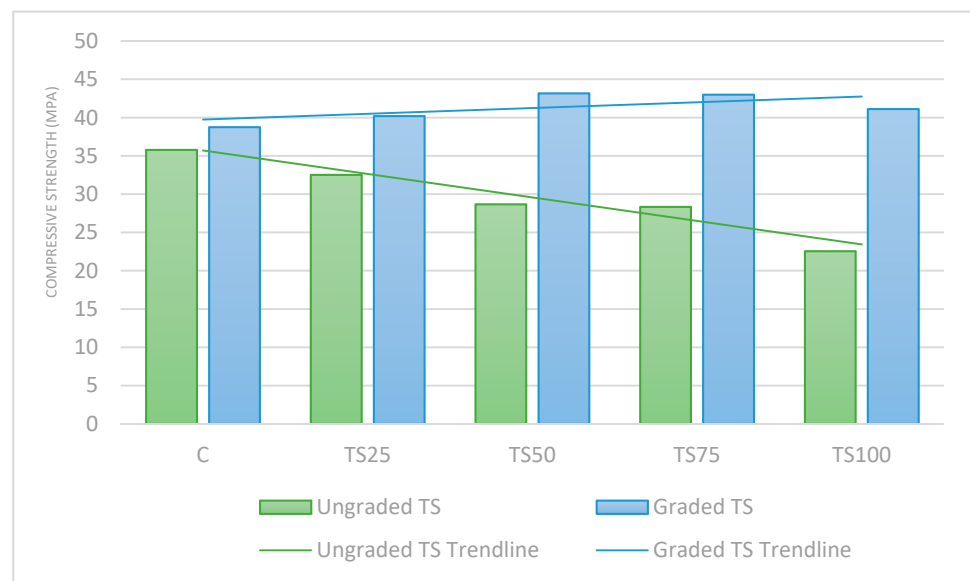


**Figure 13.** 28-day compressive strength of ungraded and graded TS mortars at a  $w/c$  of 0.55.

### 3.4. Splitting Tensile Strength

Cement composites such as mortar are generally weak while in tension. Under tension, the ITZ bears the tensile stresses for the matrix to be together. The strength of the ITZ is much weaker than that of the aggregates; thus, disintegration occurs as tensile stresses increase beyond the ITZ strength. Figure 14 shows the tensile strength of graded TS mortar samples with a  $w/c$  ratio of 0.55 at 3, 7, and 28 days. The tensile strength increased as the number of curing days increased. For example, for TS25, when the number of curing days increased from 3 days to 28 days, the tensile strength increased from 3.08 MPa to 4.1 MPa. The tensile strengths obtained at 28 days were similar for all the TS and control samples. The control sample C, TS25, and TS50 achieved tensile strengths of 4.08 MPa, 4.1 MPa, and 4.15 MPa, respectively. Similar findings were observed after 7 days of curing in all considered samples. However, after 3 days of curing, the tensile strength increased for TS25 and TS50, but decreased to values close to the control sample C. The 3-day tensile strength increased from 2.63 MPa for TS0 up to 3.08 MPa for TS50, and afterwards there was a decline to 2.62 and 2.57 for the TS75 and TS100 mortars, respectively. The higher tensile strength observed in the TS50 mix was due to the greater contribution of the hardness effect by natural sand and the bonding effect in TS when compared to other mixes. However, Waheed [38] observed a significant 35% increase in concrete strength over the control, when 20% of TS was used for sand replacement. Therefore, the gains in strength in relation to aggregates might slightly differ from mortar because of the involvement of coarse aggregates in concrete.

### 3.5. Flexural Strength

Flexural strength is sensitive to the aggregate type and little variations in specimen preparation and testing. Figure 15 shows the results of the flexural strength test of the graded TS mortar samples. The test was conducted on the TS and control samples after 3, 7, and 28 days of water curing. It was observed that, as the curing days increased, the flexural strength increased for the control and for all TS samples. Flexural strength gain of 11% to 15% was recorded from 7 to 28 days curing periods across all replacement levels. In addition, it was observed that the flexural strength increased as TS levels increased up to 75%, but peaked at 50%. However, a further increase in TS (TS100) resulted in decreased flexural strength. At 28 days of curing, the flexural strengths of TS25, TS50, TS75 and TS100

were 12.00 MPa, 12.35 MPa, 11.79 MPa and 11.48 respectively, whereas the control sample was 11.54 MPa. This shows that compressive strength at all replacement levels up to 100% were comparable to the control. The bond properties of the TS mortar matrix are influenced by the irregular and elongated aggregate shape.

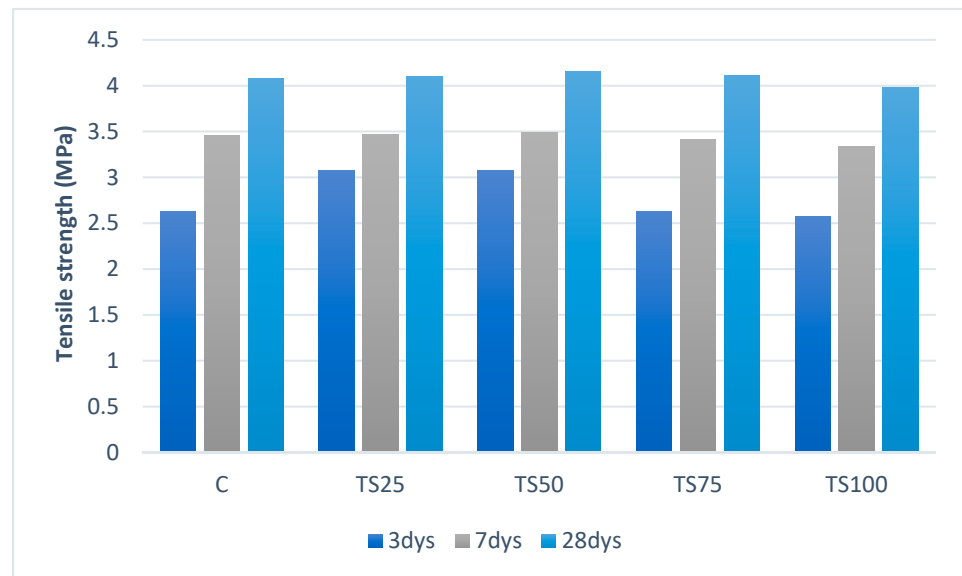


Figure 14. The tensile strength across curing days at a  $w/c$  of 0.55.

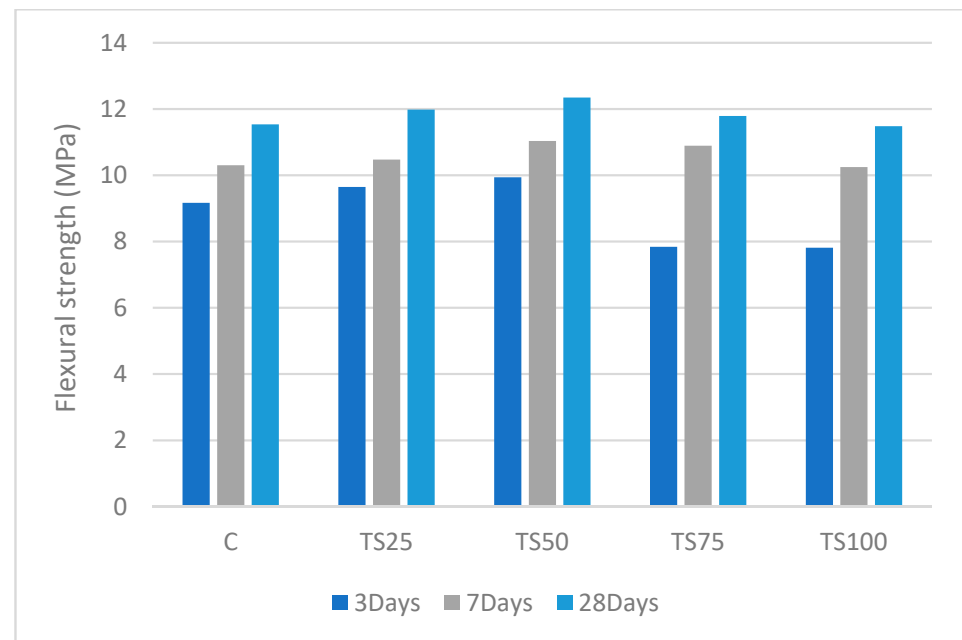


Figure 15. Flexural strength of mortars with a  $w/c$  of 0.55 at 3, 7, and 28 days of curing.

The angularity and distribution of aggregates in the cement paste played a significant role in the process of load transfer [39]. In normal-strength concrete, cracks are mostly propagated around the aggregate particles [40]. Thus, a stronger ITZ and aggregate particle interlocking in TS mortar reduces the impact on the failure plane as the stresses induced are distributed.

#### 4. Conclusions

This study was undertaken in order to evaluate the performance of TS mortar at different TS replacements. The findings show that TS aggregate can be used to replace NFA. Based on the findings of this experimental research, the following conclusions are drawn:

- Grading has a great effect on the fresh properties of TS mortar. Ungraded mortar was observed to have reduced workability as TS replacement increased, whereas grading improved the workability and reduced the water demand of graded TS mortar.
- Mortar containing 50% showed higher compressive strength than the reference mortar at all ages. Additionally, TS100 mortars had a compressive strength comparable to the control.
- The splitting tensile and flexural strengths of tin slag mortars were higher than the corresponding control mortars.
- The expansions of TS mortars were below allowable limits of 0.1%.
- TS could be used as a substitute for natural sand for the production of mortars. This would minimize cost and natural resource depletion, thus engendering the sustainability of fine aggregate.

**Author Contributions:** N.O.: Investigation and Writing—original draft; A.R.M.S.: Supervision, review/editing and funding acquisition; N.H.A.S.L.: Supervision and funding acquisition; M.A.: Writing—review & editing; I.M.: Writing—review & editing; O.A.: Writing—review & editing. All authors have read and agreed to the published version of the manuscript.

**Funding:** This research was funded by CRG grant: R.J130000.7309.4B554.

**Data Availability Statement:** Data can be made available from the authors.

**Conflicts of Interest:** The authors declare no conflict of interest.

#### References

1. Klee, H. The cement sustainability initiative. *Cem. Sustain. Initiat.* **2017**, *157*, 9–12.
2. Li, H.; Huang, F.; Cheng, G.; Xie, Y.; Tan, Y.; Li, L.; Yi, Z. Effect of granite dust on mechanical and some durability properties of manufactured sand concrete. *Constr. Build. Mater.* **2016**, *109*, 41–46. [[CrossRef](#)]
3. Makhloufi, Z.; Kadri, E.H.; Bouhicha, M.; Benaissa, A.; Bennacer, R. The strength of limestone mortars with quaternary binders: Leaching effect by demineralized water. *Constr. Build. Mater.* **2012**, *36*, 171–181. [[CrossRef](#)]
4. Zhao, Z.; Qu, X.; Li, F.; Wei, J. Effects of steel slag and silica fume additions on compressive strength and thermal properties of lime-fly ash pastes. *Constr. Build. Mater.* **2018**, *183*, 439–450. [[CrossRef](#)]
5. Ogundiran, M.B.; Nugteren, H.W.; Witkamp, G.J. Immobilisation of lead smelting slag within spent aluminate-fly ash based geopolymers. *J. Hazard. Mater.* **2013**, *248–249*, 29–36. [[CrossRef](#)]
6. Prem, P.R.; Verma, M.; Ambily, P.S. Sustainable cleaner production of concrete with high volume copper slag. *J. Clean. Prod.* **2018**, *193*, 43–58. [[CrossRef](#)]
7. Prasad, V.D.; Prakash, E.L.; Abishek, M.; Dev, K.U.; Kiran, C.K.S. Study on concrete containing Waste Foundry Sand, Fly Ash and Polypropylene fibre using Taguchi Method. *Mater. Today Proc.* **2018**, *5*, 23964–23973. [[CrossRef](#)]
8. Tamanna, N.; Tuladhar, R.; Sivakugan, N. Performance of recycled waste glass sand as partial replacement of sand in concrete. *Constr. Build. Mater.* **2020**, *239*. [[CrossRef](#)]
9. Pandey, P.; Harison, A.; Srivastava, V. Utilization of Waste Foundry Sand as Partial Replacement of Fine Aggregate for Low Cost Concrete. *Inpressco* **2015**, *5*, 3535–3538.
10. Kashani, A.; Ngo, T.D.; Hajimohammadi, A. Effect of recycled glass fines on mechanical and durability properties of concrete foam in comparison with traditional cementitious fines. *Cem. Concr. Compos.* **2019**, *99*, 120–129. [[CrossRef](#)]
11. Izard, C.F.; Müller, D.B. Tracking the devil's metal: Historical global and contemporary U.S. tin cycles. *Resour. Conserv. Recycl.* **2010**, *54*, 1436–1441. [[CrossRef](#)]
12. Shakil, U.A.; Bin, S.; Hassan, A. Behavior and properties of tin slag polyester polymer concrete confined with FRP composites under compression. *J. Mech. Behav. Mater.* **2020**, *29*, 44–56. [[CrossRef](#)]
13. Hashim, M.J.; Mansor, I.; Ismail, M.P.; Sani, S. Preliminary study of tin slag concrete mixture. In Proceedings of the IOP Conference Series: Materials Science and Engineering, International Nuclear Science, Technology and Engineering Conference 2017 (iNuSTEC2017), Selangor, Malaysia, 25–27 September 2017; Volume 298. [[CrossRef](#)]
14. Rustandi, A.; Nawawi, F.; Cahyadi, A. Evaluation of the suitability of tin slag in cementitious materials: Mechanical properties and Leaching behaviour Evaluation of the suitability of tin slag in cementitious materials: Mechanical properties and Leaching

- behaviour. In Proceedings of the IOP Conference Series: Materials Science and Engineering, International Conference on Chemistry and Material Science (IC2MS) 2017, Malang, Indonesia, 4–5 November 2017; Volume 299. [\[CrossRef\]](#)
15. ASTM International, Standard Test Methods for Chemical Analysis of Hydraulic Cement<sup>1</sup>. 2004; Volume i, 1–31.
  16. ASTM International, Standard Test Method for Density, Relative Density (Specific Gravity), and Absorption. 2004; 1–6.
  17. ASTM International, Standard Specification for Concrete Aggregates. 2001; Volume 04.
  18. ASTM International, Standard Test Method for Flow of Hydraulic Cement Mortar. 2013; 1–2. [\[CrossRef\]](#)
  19. ASTM International, Standard Test Method for Compressive Strength of Hydraulic Cement Mortars. 2005; Volume 04, 1–6.
  20. ASTM International, Standard Test Method for Splitting Tensile Strength of Cylindrical Concrete Specimens. 2006; 4–8.
  21. ASTM International, Standard Test Method for Flexural Strength of Hydraulic-Cement Mortars. 1998; Volume 04, 2–7.
  22. Youness, D.; Yahia, A.; Tagnit-Hamou, A. Coupled rheo-physical effects of blended cementitious materials on wet packing and flow properties of inert suspensions. *Constr. Build. Mater.* **2020**. [\[CrossRef\]](#)
  23. Estephane, P.; Garboczi, E.J.; Bullard, J.W.; Wallevik, O.H. Three-dimensional shape characterization of fine sands and the influence of particle shape on the packing and workability of mortars. *Cem. Concr. Compos.* **2019**, *97*, 125–142. [\[CrossRef\]](#)
  24. Wu, W.; Zhang, W.; Ma, G. Mechanical properties of copper slag reinforced concrete under dynamic compression. *Constr. Build. Mater.* **2010**, *24*, 910–917. [\[CrossRef\]](#)
  25. Abdel-Magid, T.I.M.; Hamdan, R.M.; Abdelgader, A.A.B.; Omer, M.E.A.; Ahmed, N.M.R.A. Effect of Magnetized Water on Workability and Compressive Strength of Concrete. *Procedia Eng.* **2017**, *193*, 494–500. [\[CrossRef\]](#)
  26. Praveen Kumar, K.; Radhakrishna, X.X. Workability Strength and Elastic Properties of Cement Mortar with Pond Ash as Fine Aggregates. *Mater. Today Proc.* **2020**, *24*, 1626–1633. [\[CrossRef\]](#)
  27. Westerholm, M.; Lagerblad, B.; Silfwerbrand, J.; Forssberg, E. Influence of fine aggregate characteristics on the rheological properties of mortars. *Cem. Concr. Compos.* **2008**, *30*, 274–282. [\[CrossRef\]](#)
  28. Cu, Y.T.H.; Tran, M.V.; Ho, C.H.; Nguyen, P.H. Relationship between workability and rheological parameters of self-compacting concrete used for vertical pump up to supertall buildings. *J. Build. Eng.* **2020**, *32*. [\[CrossRef\]](#)
  29. Pauzi, N.N.M.; Jamil, M.; Hamid, R.; Abdin, A.Z.; Zain, M.F.M. Influence of spherical and crushed waste Cathode-Ray Tube (CRT) glass on lead (Pb) leaching and mechanical properties of concrete. *J. Build. Eng.* **2019**, *21*, 421–428. [\[CrossRef\]](#)
  30. Edwin, R.S.; Gruyaert, E.; De Belie, N. Influence of intensive vacuum mixing and heat treatment on compressive strength and microstructure of reactive powder concrete incorporating secondary copper slag as supplementary cementitious material. *Constr. Build. Mater.* **2017**, *155*, 400–412. [\[CrossRef\]](#)
  31. ASTM Standard Test Method for Potential Alkali Reactivity of Cement-Aggregate Combinations (Mortar-Bar Method). *Annu. B ASTM Stand.* **2003**, *i*, 1–5.
  32. Piasta, W.; Zarzycki, B. The effect of cement paste volume and  $w/c$  ratio on shrinkage strain, water absorption and compressive strength of high performance concrete. *Constr. Build. Mater.* **2017**, *140*, 395–402. [\[CrossRef\]](#)
  33. Rahmani, K.; Shamsai, A.; Saghafian, B.; Peroti, S. Effect of Water and Cement Ratio on Compressive Strength and Abrasion of Microsilica Concrete. *Middle East J. Sci. Res.* **2012**, *12*, 1056–1061. [\[CrossRef\]](#)
  34. Sipil, T.; Teknik, F.; Tengah, S.; Teknik, F.; Tengah, S. The effect of coarse aggregate hardness on the fracture toughness and compressive strength of concrete. *MATEC Web Conf.* **2019**, *258*, 04011.
  35. Ouda, A.S.; Abdel-gawwad, H.A. The effect of replacing sand by iron slag on physical, mechanical and radiological properties of cement mortar. *HBRC J.* **2017**, *13*, 255–261. [\[CrossRef\]](#)
  36. Guo, Y.; Xie, J.; Li, J. Effect of steel slag as fine aggregate on static and impact behaviors of concrete. *Constr. Build. Mater.* **2018**, *192*, 194–201. [\[CrossRef\]](#)
  37. Li, L.G.; Lin, C.J.; Chen, G.M.; Kwan, A.K.H.; Jiang, T. Effects of packing on compressive behaviour of recycled aggregate concrete. *Constr. Build. Mater.* **2017**, *157*, 757–777. [\[CrossRef\]](#)
  38. Waheed, A. Properties of Concrete Containing Effective Microorganisms Using Tin Slag as Fine Aggregate Replacement. Master's Thesis, Universiti Teknologi Malaysia, Johor, Malaysia, 2018.
  39. Maitra, S.R.; Reddy, K.S.; Ramachandra, L.S. Load Transfer Characteristics of Aggregate Interlocking. *J. Transp. Eng.* **2010**. [\[CrossRef\]](#)
  40. Darwin, D.; Kozul, R. *Effects of Aggregate Type, Size, and Content on Concrete Strength and Fracture Energy*; SM Report No. 43, University of Kansas Center for Research, Inc.: Lawrence, KS, USA, 1997.